Remote Sensing and Landslide Hazard Assessment*

J. McKean
USDA Forest Service, Pleasant Hill, CA 94523
S. Buechel
TGS, Inc., NASA Ames Research Center, Moffett Field, CA 94035
L. Gaydos
U. S. Geological Survey, NASA Ames Research Center, Moffett Field, CA 94035

ABSTRACT: Remotely acquired multispectral data are used to improve landslide hazard assessments at all scales of investigation. A vegetation map produced from automated interpretation of TM data is used in a GIS context to explore the effect of vegetation type on debris flow occurrence in preparation for inclusion in debris flow hazard modeling. Spectral vegetation indices map spatial patterns of grass senescence which are found to be correlated with soil thickness variations on hillslopes. Grassland senescence is delayed over deeper, wetter soils that are likely debris flow source areas. Prediction of actual soil depths using vegetation indices may be possible up to some limiting depth greater than the grass rooting zone. On forested earthflows, the slow slide movement disrupts the overhead timber canopy, exposes understory vegetation and soils, and alters site spectral characteristics. Both spectral and textural measures from broad band multispectral data are successful at detecting an earthflow within an undisturbed old-growth forest.

INTRODUCTION

AMONG NATURAL HAZARDS, landslides are one of the most costly and damaging. For example, Schuster (1978) estimates that direct and indirect losses from landslides in the U.S.A. are approximately $1 billion per year. Similar levels of damage have been noted throughout the world where mountainous terrain exists. Landslide damage occurs as loss of life, property damage, and environmental damage, the latter primarily as sedimentation into streams and lakes. The mechanics of individual landslides are well understood. The likelihood of failure of a single landslide can be analyzed using deterministic limit equilibrium methods based upon the principles of soil mechanics. However, definition of the material properties and site conditions needed for such a failure analysis are difficult and costly to obtain, even at a single site. Furthermore, these are static analyses that only give an estimate of whether or not a slide should occur at a site under specific environmental conditions. They cannot be used to assess the activity or rate of movement of a slide after it begins to fail. Average slide movement rates can only be established by repeated ground surveys over periods of months to years.

If landslide hazard assessment is done over larger areas than a single site, then a traditional deterministic slope stability analysis is still more difficult because of the need to characterize both temporal and spatial variability in the site conditions. Some investigators then use geomorphological approaches in which landforms in a local area and the processes that formed them are defined. Landforms whose history includes the occurrence of landslides are then mapped as probable sources of future slides. When evaluating even larger regions, some workers also employ multivariate statistical methods to search for critical combinations of site conditions such as soil characteristics, degree of slope, bedrock type, rainfall/snowmelt conditions, and vegetative cover that correlate well with the past occurrence of landslides. Once the critical combinations of conditions are identified, their spatial distribution may be mapped into displays of relative landslide susceptibility. Both the statistical and geomorphic process approaches require the mapping of terrain characteristics over large areas.

Regardless of the scale of investigation, all landslide hazard assessment techniques rely on evaluation of site conditions. The inherent spatial variability of conditions at all scales greatly complicates sampling and accurately mapping these factors. Remote sensing methods, with their ability to view large areas synoptically, have the potential to improve site condition mapping and thus slide hazard assessment. A summary is presented here of work in progress to evaluate the use of remote sensing techniques to improve debris flow and earthflow landslide hazard assessment at a variety of scales.

In the first case, remote sensing data are used to map vegetation for input as a data layer in a multifactor analysis of landslide susceptibility mapping in San Mateo County, California. In the next example, remote sensing methods are employed to map vegetation phenologic patterns and, thus indirectly, debris flow-susceptible landforms defined based on local geomorphic processes. In this research multispectral data from a test site in Marin County, California are used to detect and map hillslope deposits of colluvium that are primary debris flow source areas. The synoptic perspective of remote sensing provides a unique way to apply such physically based landform mapping over larger areas. Finally, remote sensing is used to provide new data for site specific evaluations of both landslide extent and level of activity as demonstrated for the case of earthflows obscured by an old-growth coniferous forest in central Oregon. The locations of the three study areas are shown in Figure 1.

VEGETATION MAPPING AND DEBRIS FLOWS

INTRODUCTION

Following severe storms in 1982, over 4,000 debris flows occurred in the San Francisco Bay Area, resulting in 25 deaths and extensive property damage (Ellen and Wieczorek, 1988). This initiated a U.S. Geological Survey sponsored effort to produce a digital database for San Mateo County to be used in understanding and predicting geological hazards (Brabb, 1987). Using this database, a logit regression model was developed and used to produce a debris flow probability map based on

*Presented at the Eighth Thematic Conference on Geologic Remote Sensing, Denver, Colorado, 29 April–2 May 1991.

PHOTOGRAMMETRIC ENGINEERING & REMOTE SENSING,
Vol. 57, No. 9, September 1991, pp. 1185–1193.

0099-1112/91/5709–1185$03.00/0

storm rainfall, soil categories, slope, and mean annual rainfall (Mark, in press). A forest/non-forest stratification was used to correct the model for reduced debris flow mapping accuracy in forested area; however, vegetation *per se* was not included. Vegetation is considered a potentially relevant factor in cases of shallow sliding such as debris flows, although concrete evidence in support of a specific relationship is difficult to find in the literature. Vegetation mapping is well suited to remote sensing techniques, and a vegetation map was produced using Landsat Thematic Mapper data for evaluation as input to a small-scale assessment of debris flow hazard. Vegetation is being considered both as a physical variable, and as a predictor of other factors important to hazard assessment such as soil type. Results from consideration of vegetation as a physical factor are presented here.

The potential role of vegetation in influencing debris flow occurrence and character is well understood in the context of a large-scale physical model; however, the necessary input parameters such as root strength and detailed soil depth are difficult to measure. Failures tend to develop below the root zone, so variation in vegetation rooting depth should affect the size and shape of debris flows. In the case of shallow soils with roots penetrating bedrock, vegetation may even affect the occurrence of debris flows (Reneau, 1988). Among the factors to be considered, general rooting depth and vegetation water-use habits are identifiable at vegetation (versus floristic) scales and may be assumed to influence debris flow character. Vegetation types for classification were selected based on gross differentiation of these factors. For San Mateo County, with a Mediterranean climatic regime, the classes included (parentheses note indicator plants for the associations) grasslands, coastal scrub (Artemesia californica, Baccharis pilularis), chamise chaparral (Adenostoma fasiculatum), redwoods (Sequoia sempervirens), other conifers (Pseudotsuga menziesii), and mixed evergreen forest (Quercus agrifolia, Lithocarpus densiflorus, Aesculus californica, Umbellularia californica, Arbutus menziesii).

Classification

A multi-date supervised classification was used to produce the vegetation map. Known training sets of the selected vegetation associations were evaluated for separability using transformed divergence. Two dates of Landsat TM data representing local seasonal extremes—8 July 1985 and 26 March 1988—were used for developing statistics. TM bands 1, 4/3, 5/4, and 6 from each date were found to provide the greatest overall separability. A maximum-likelihood classification was performed using in-house software in a workstation environment. Confused classes were clustered and reclassified using an iterative nearest neighbor clustering routine to further maximize separability. The accuracy of the final map was tested using a stratified random sampling and an assumed accuracy level of 85 percent (510 points). The mapped classes were checked against 1985 1:45,000-scale CIR photography combined with field checks where possible. The resulting Kappa coefficient of agreement was 95 percent overall.

The vegetation map was combined with the USGS data layers for soils (USGS Hillside Materials Map), slope angle and aspect maps generated from a 30-m DEM, and the debris flow occurrence map from the 1982 storm (Figure 2). Overlay analysis software was used to extract debris flow frequencies for desired classes using the entire data set.

Results

The debris flow frequency for the vegetation classes as a whole follows the expected trend if general rooting depth alone is considered. In decreasing order of debris flow occurrence the following gradient was noted: coastal scrub (7 percent), grassland (6.74 percent), chaparral (3.33 percent), mixed evergreen forest (2.80 percent), redwoods (2.04 percent), and other conifers (1.89 percent). Vegetation distribution, however, varies with soil type and topographic parameters as does debris flow potential. Figure 3 illustrates differences found in the mean and standard deviation between the vegetation classes by soil group. In order to separate these factors and focus on vegetation effects, the granitic soil category was selected for further detailed

FIG. 1. Location map.

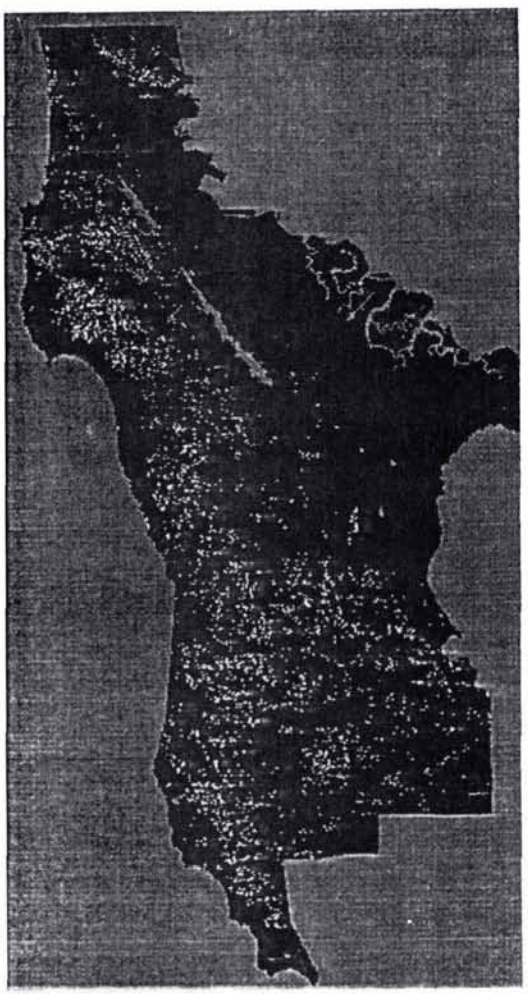

FIG. 2. San Mateo County, California. Debris flow mapping, January 1982 storm.

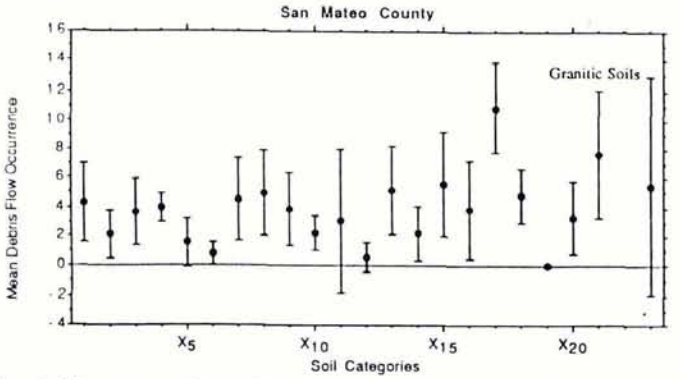

FIG. 3. The mean and standard deviation of debris flow occurrence over all vegetation classes for each of the 23 USGS mapped soil categories suggest a varied vegetation response. Details are presented for class 24, granitic soils.

analysis. This soil group has a high degree of variation in the debris flow frequency of the vegetation, a large sample size, and a generally accepted high hazard of debris flows. Figure 4 illustrates the within slope/aspect relationships for the four vegetation classes which had sufficient area for analysis within granitic soils. In keeping with the contradictions of past literature, both similarities and differences are apparent. All vegetation irrespective of type has the lowest flow frequency on slopes 4 to 14 degrees with a north to northeast aspect, and a peak frequency at slopes of 24 to 34 degrees with a west/northwest aspect (slopes steeper than 34 degrees are not included due to small sample size). The greatest differences between vegetation types occur, on all slopes, in the drier south to east aspects, with grassland and coastal scrub debris flow frequencies consistently higher than the forested categories. Although the greatest differences among vegetation types are on the driest aspects, the shallower rooted vegetation shows less slope/aspect response overall. If the assumption is made that deeper roots, given similar soils, will increase the shear strength, thus requiring greater pore pressure for failure, this effect would be expected. The shallow rooted vegetation, again holding other factors constant, more readily surpasses lower shear strength/pore pressure limits, resulting in a more consistent response over topographic variation. The reduction in debris flows to the north/northeast for all vegetation types appears to be a site- or storm-specific phenomenon requiring further study. Due to undersampling of debris flows under forest cover, it is difficult to draw conclusions regarding the absolute reduced occurrence evident in tree cover; however, the shape of the response surface should remain constant.

Although many variables known to influence debris flow hazard are not available for small-scale mapping, a simplified model appears to describe a supportable response of vegetation, apart from several major confounding factors. The findings will be tested within other soil types. This information will be used in testing the current logit regression model for enhanced predictability, as well as in designing an expert system approach, well suited to incorporating the uncertainty inherent in the generalizations necessary for regional scale hazard mapping.

GRASSLAND SENESCENCE AND DEBRIS FLOWS

INTRODUCTION

On hillslopes mantled by relatively coarse-grained soils, rapid and catastrophic debris flow landslides often occur in response to groundwater peaks. Past research has shown that such soil mantles are usually not of uniform thickness but, rather, colluvial soil is concentrated in fairly regularly spaced depressions in the underlying bedrock (Hack and Goodlett, 1960; Dietrich and Dunne, 1978). These depressions have been termed "hollows," and the intervening area between two adjacent hollows is known as a "nose" because of the convex outward topography at such locations. Hollows typically are small unchanneled valleys about 75 metres wide by several hundred metres long. The colluvial deposits in the hollows can reach several metres in depth while soil thicknesses on noses are generally less than 0.5 metres. Because of the greater thickness of colluvium in the hollows and the topographically induced surface and groundwater concentration there, these sites have been recognized as primary sources of debris flows (Dietrich *et al.*, 1987). When the hollows are filled with colluvium, they have little topographic expression and are difficult to locate and map as must be done to properly evaluate the aerial distribution of debris flow hazard.

In the San Francisco Bay region of California many hillslopes composed of noses and hollows support grassland vegetative cover. The phenology of grasslands in this portion of California is driven by seasonal climatic variations that include a wet winter season from October through April followed by extreme drought for the remainder of the year. Following growth initiation in the fall, the grasses grow slowly until spring, then experience rapid growth until the soil moisture falls during the early portion of the year drought (Chiariello, 1989). At that point the grasses reproduce and die or become dormant through the summer. Grassland senescence in the deeper hollow soils is delayed, possibly due to the increased moisture availability of the deeper colluvial deposits later in the season. Differentiating patterns of grass senescence using remotely sensed data allows the opportunity to relate locations of delayed senescence to likely debris flow sites in thicker colluvial deposits.

Using field sites in Marin County, California, a study has been initiated to investigate the utility of multispectral data to locate and define these potential debris flow source areas on grass-covered slopes. Thematic Mapper Simulator NS001 data were acquired with a nadir resolution of about 2.5 metres on four dates during the 1989 grassland growing season (April to June). Targets were placed in the field to allow precise registration of the overflights. During all overflights, ground sampling was conducted to evaluate soil and grass canopy moisture conditions on noses and hollows.

The broad-band spectral characteristics of senescing graminae vegetation have been documented in the context of crop and rangeland assessment. The breakdown of chlorophyll results in a decrease in absorption in the red range (0.6 to 0.7 μm) (Heilman and Boyd, 1986; Miller et al., 1984; Huete and Jackson, 1987). A decrease in moisture content reduces the absorption in the mid-infrared wavelengths (Hunt *et al.*, 1987). Many vegetation indices have been developed to exploit these characteristics for estimating biomass and leaf area index (LAI) with the presence of dormant vegetation considered a confounding factor. Three vegetation indices, selected for their response to different portions of the spectral range, were evaluated for their ability to differentiate patterns of grassland senescence relevant to variation in soil depth. These include

- near-infrared/red (Band 4/Band 3) - IR/R,
- mid-infrared/infrared (Band 6/Band 4) — MIR/IR, and
- "greeness" - derived from a Karhunen-Loeve transformation using the first seven NS001 bands on a subset of grass and soil data.

These indices were calculated for all image dates at a site known as Solstice (Figure 5) where detailed topographical and soil thickness data are available from the research of Wilson (1988) and Dengler *et al.* (1987) (Figure 7). In addition, a measure of seasonal change was calculated using the first eigenvector of the IR/R indices across the four dates sampled.

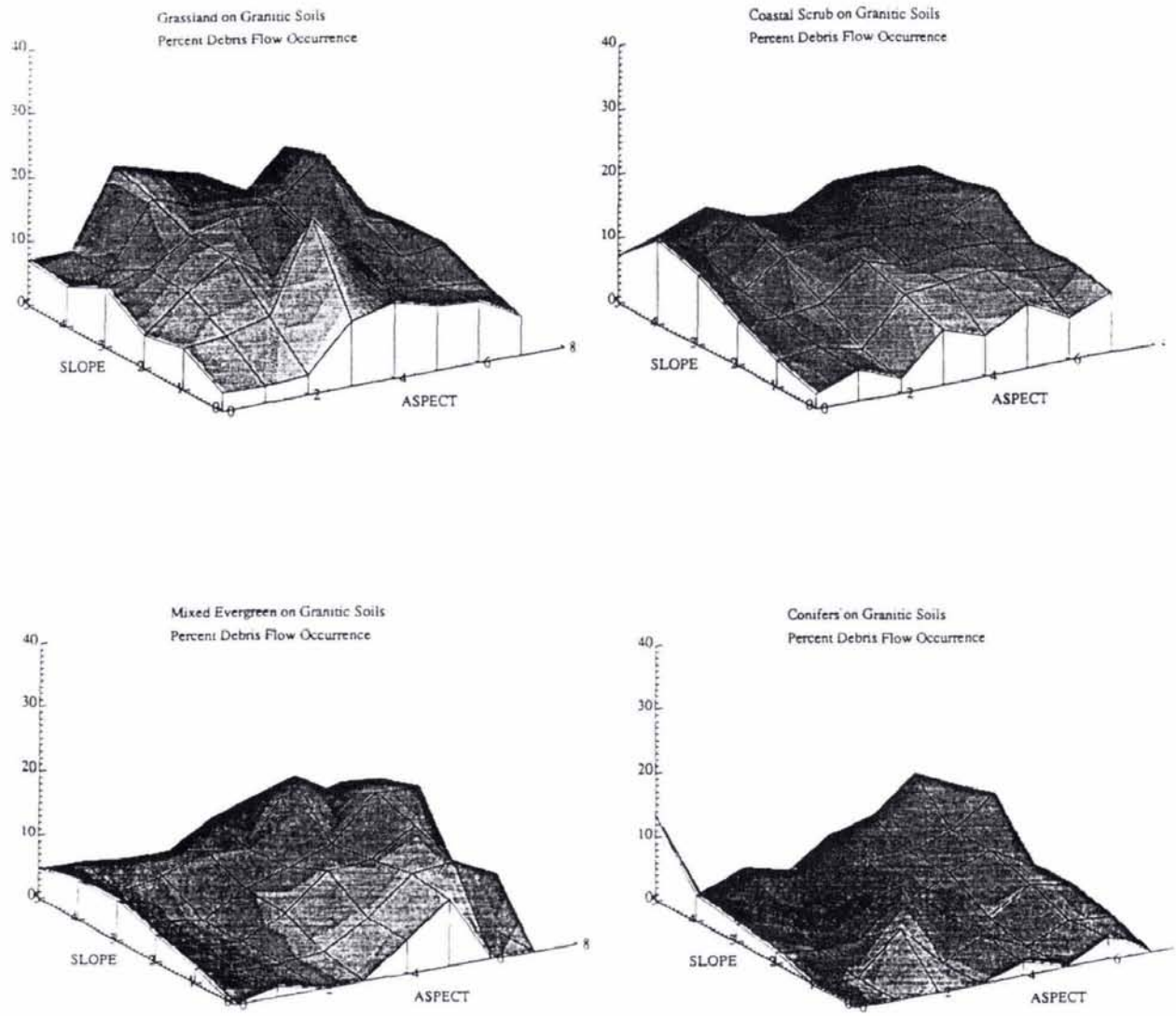

FIG. 4. Debris flow occurrence within soil, vegetation, slope, and aspect categories. Aspect (0–7) runs clockwise from the north; slope codes in degrees – (0) 4–9, (1) 10–14, (2) 15–19, (3) 20–24, (4) 25–29, (5) 30–34.

RESULTS

The ground data indicate that at the Solstice site the thin soils on the noses are drier throughout the April to June period (Table 1). The relative water content of the grasses, however, does not begin to diverge into separable nose and hollow populations until the 18 May sample date.

By 18 May, all three spectral indices delineate separate nose/hollow populations. Stratifications based on the cluster values produce maps which correspond well with gross change in soil depth (Figure 6). Differences between indices in the stratifications are slight but potentially significant. For example, indices varied in mapping of a small concavity along the margin of one nose at Solstice, suggesting a localized pocket of deeper colluvium. The change index was equally successful at delineating nose versus hollow and produced greater differentiation among shallower soils. Studies are continuing to evaluate the accuracy, causes, and possible physical significance of these differences in the details of the stratifications.

Transects were made across the Solstice area, and the vegetation indices were regressed against measured soil depths. The agreement between the indices on or after 18 May and the soil depths is quite good up to depths of a few metres. Transect T-T′ in Figure 8 is an example using the greeness index calculated for 18 May 1989. The location of Transect T-T′ is shown in Figure 7. The regression equation developed from this index on the transect is significant at less than the 1 percent level with an $R^2 = 0.60$. Beyond colluvium depths of a few metres these relationships break down because of the limited rooting depth of the grasses.

The methodology is successful in detecting and mapping the limits of colluvial deposits in hollows with a grass cover. The advantage of such a technique is that it allows rapid survey over large areas of potential debris flow sites. Done at a reconnaissance level, information derived could be used to focus field work in suspect areas and thus greatly increase the efficiency of debris flow hazard surveys. Investigations are continuing to test the methodology at other sites, identify sources of error, and evaluate the ability to predict actual soil depths at other locations.

FORESTED EARTHFLOWS

INTRODUCTION

When weak fine-grained soils and rocks with poor drainage properties occur on hillslopes, slow persistent landsliding in the

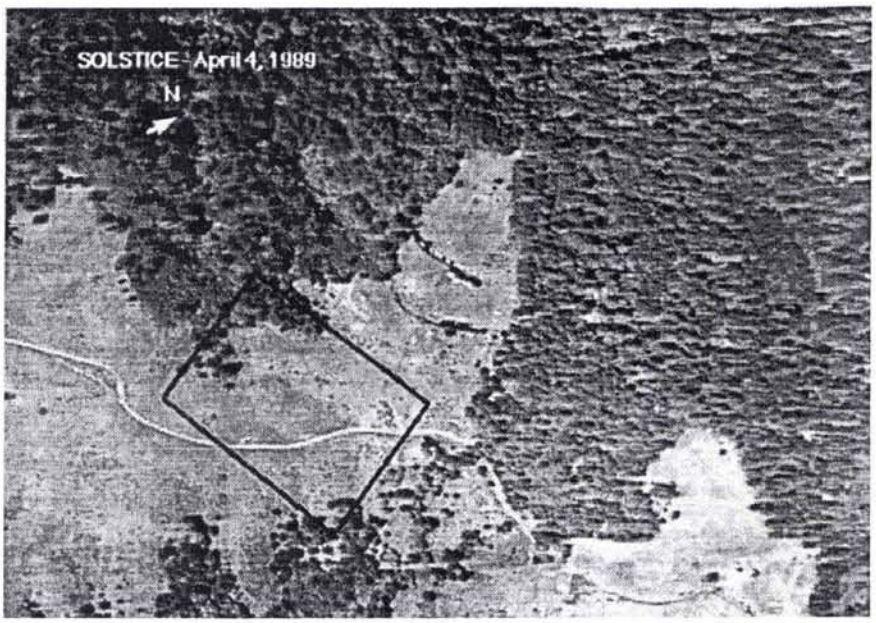

FIG. 5. Solstice site, Marin County, California. NS001 band 6, mid-infrared, approximate scale of original, 1:20,000.

TABLE 1. SOIL AND VEGETATION MOISTURE—MARIN COUNTY 1989

	4 April	27 April	18 May	8 June
Soil Average Moisture (%)				
Noses ($n=9$)	21 ± 4	15 ± 3	4 ± 2	6 ± 2
Hollows ($n=12$)	38 ± 15	21 ± 5	12 ± 4	12 ± 4
Vegetation Relative Water Content (%)				
Noses ($n=9$)	80 ± 9	76 ± 6	65 ± 7	60 ± 1
Hollows ($n=12$)	81 ± 7	78 ± 4	75 ± 7	75 ± 8

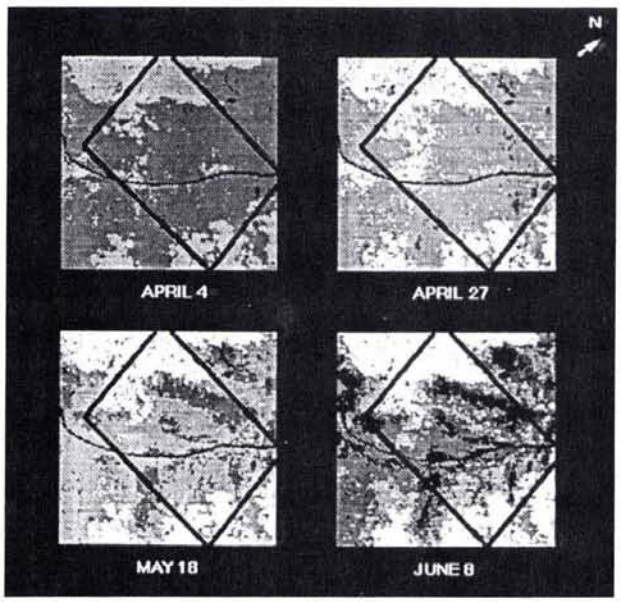

FIG. 6. Four-class stratification mapping of senescence using IR/R across the 1989 season. Color coding ranges from darkest (least "green") to lightest (most "green").

form of earthflows is very common. For example, one study of clay-rich soils derived from weathered volcanic rocks in the

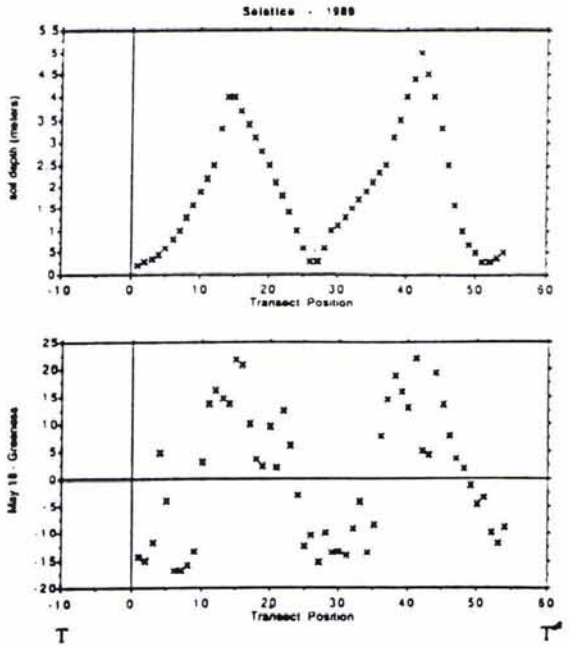

FIG. 8. Transect T-T'. Soil depths and 18 May 1989 greeness values.

western Cascade Mountains of Oregon found that earthflows cover more than 25 percent of such hillslopes (Swanson and James, 1975). Individual flows range in surface area from hectares to several square kilometres. These slides resemble glaciers in both their appearance and style of movement. In response to seasonal or longer groundwater fluctuations, earthflows creep downslope at typical rates of centimetres to metres per year. While not catastrophic, these rates are sufficient to seriously affect engineering structures such as roads and bridges. Earthflows are also a major souce of sediment mobilized on hillslopes and transported into streams as noted by Kelsey (1977).

On forested earthflows, the forest canopy is often rafted

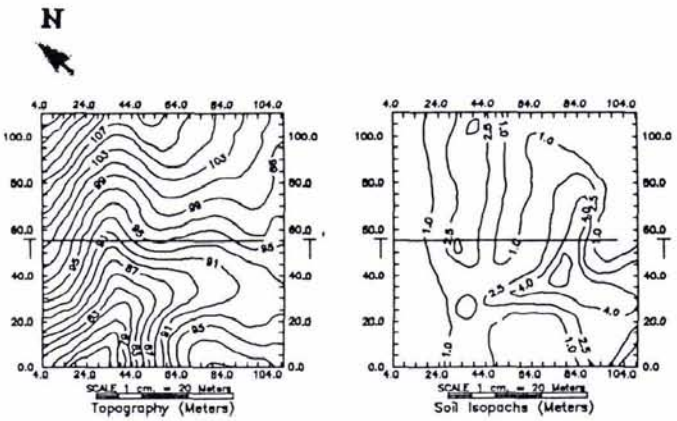

FIG. 7. Solstice site.

downslope on top of the slides with only minor to moderate disturbance. The canopy obscures the slides and makes them difficult to detect and evaluate on airphotos. Partial disruption of a coniferous canopy by an earthflow changes the size, frequency, and shape of openings or gaps in the tree cover. Deciduous vegetation, other ground cover, and bare soil with spectral characteristics different from conifers are then exposed to overhead sensors. The amount and spatial pattern of the canopy gap-associated spectral reflectance changes may be used alone or in conjunction with ancillary data to screen large forested areas for the presence of earthflows. Furthermore, the degree of canopy disruption is a function of the level of activity or velocity of an earthflow. Remote spectral data may therefore be used to estimate the velocity of an earthflow or to define areas within a flow moving at different rates and thus evaluate the internal mechanics of a slide.

These ideas are being tested at known earthflows in the Cascade Mountains of Oregon with the primary test site at the Jude Creek, Oregon earthflow (Figure 1). At Jude Creek the canopy is an old growth Douglas-fir (Pseudotsuga menziesii) and Western Hemlock (Tsuga heterophylla) forest. Previous studies (Lienkaemper, pers. comm.) at this earthflow have established that movement is occurring at different rates in three different zones within the slide (Figure 9). This allows testing of the ability of remotely sensed data to differentiate velocity zones within a slide. Sample plots were established on the ground in undisturbed areas outside the slide and in each of the movement zones within the slide (Figure 9). Canopy samples were taken from the plots on three dates in the summer of 1989 contemporaneous with acquisition of aircraft and satellite multispectral data. Measurements of canopy condition were also taken in the plots. Using a 5 September 1989 NS001 scanner data set with a spatial resolution of about six metres, we have begun evaluating the use of multispectral data to detect and map forested slides like the Jude Creek earthflow.

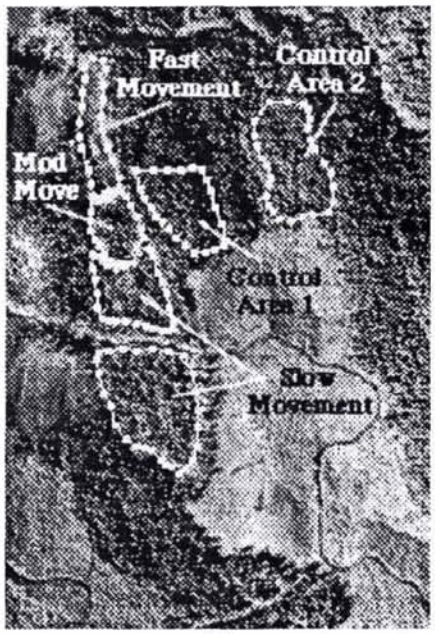

(a)

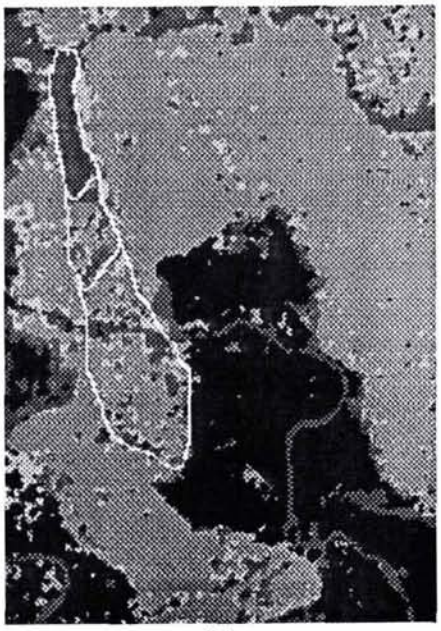

(b)

FIG. 9. Jude Creek Earthflow. Approximate scale of original, 1:16,000. (a) Location map. Slide and control areas outlined. (b) Maximum-likelihood classification. NS001 bands 2, 3, 4, 5, 6. Median filtered. Slide outlined.

RESULTS

Using large-scale airphotos, a detailed mapping of individual tree crown positions and spacing in undisturbed forest and within the earthflow reveals that there is disturbance of the canopy (Table 2). There is also a systematic increase in the amount of disturbance in proportion to the rate of slide movement. As the earthflow accelerates, the aerial percent cover of the canopy decreases and the average size of gaps in the canopy increases. The gaps also change from discrete small ovoid shapes in the undisturbed forest to elongate forms that coalesce into larger connected areas denuded of trees. At movement rates of greater than about five metres per year (fast rate), essentially all of the canopy is knocked over and vegetation is restricted to replacement deciduous species.

The canopy gaps formed at slide movement rates of less than about one metre per year (slow rate) are invaded in a few years by deciduous vegetation. This change in vegetation type and general decrease in canopy absorption cause the mean radiance to increase in all spectral bands relative to undisturbed forest with the increase being greatest in the infrared region (Figure 10). Plots of red versus infrared (Bands 3 and 4) data from the control undisturbed forest and the slow movement zone again

TABLE 2. JUDE CREEK EARTHFLOW CANOPY DISTURBANCE

Movement Category	Average Velocity Metres/year	Canopy Cover Percent	Average Gap Size Square Metres	Canopy Gap Description
Undisturbed Forest 1	0	92	100	Round, Discrete
Undisturbed Forest 2	0	89	160	Round, Discrete
Slow	0.5	70	650	Elongate
Moderate	2.5	58	~750	Large, Coalesced
Fast	7.0	4	•	No Isolated Gaps

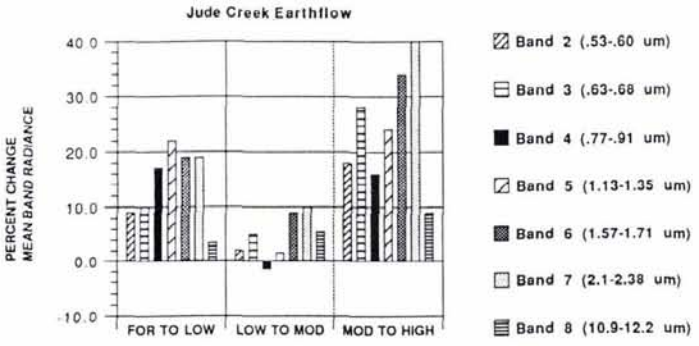

FIG. 10. Jude Creek earthflow. Percent change mean band radiances.

show a brightening, predominately in Band 4 (Figure 11). This Band 4 brightening is most dramatic around the margin of the upslope end of the slide. Here local differential ground movement has disrupted the canopy and allowed dense growth of deciduous vegetation. Elsewhere in the slow movement zone, the broad band spectral characteristics more closely resemble the undisturbed forest as might be expected from the approximately 70 percent canopy cover that remains (Table 2).

At moderate movement rates (1 to 5 metres per year), many of the Douglas fir trees and a few of the Western Hemlocks are toppled. The larger canopy gaps now formed expose deciduous undergrowth vegetation but also a considerable area of dead wood from the trunks of the fallen trees. Less than 60 percent of the area is covered by the coniferous canopy. The results of these changes in the scene background are to increase the mean mid-infrared (Bands 6 and 7) radiance relative to slow movement areas but cause little change in the near-infrared (Bands 4 and 5) (Figure 10). An increase of mid-infrared relative to near-infrared is consistent with reflectances reported in the literature for dead wood in spruce trees (Vogelmann and Rock, 1986) and brown wood from pinyon pine (Elvidge, 1990). The red radiance (Band 3) also increases relative to the near-infrared and could be explained by again the exposure of dead wood (Elvidge, 1990) or the local soils (see Figure 11 for typical local soil radiances obtained from exposures in an abandoned quarry adjacent to the earthflow).

At slide rates greater than five metres per year, the original canopy has been virtually destroyed and bare soil and deciduous vegetation dominate the scene. Mean reflected band radiances all increase by 15 percent to 40 percent (Figure 10) with the largest increases in the red and mid-infrared (Bands 3,6,7). The scatter plot of Band 4 and Band 3 data also shows an increased spread toward the values for local soils (Figure 11).

Using the Jude Creek earthflow individual movement rate zones as training areas to generate spectral statistics, a supervised maximum-likelihood classification was performed (Figure 9; Note: the classification in Figure 9 has been median filtered). This classification appears to have been able to detect and define the limits of the earthflow. Commission errors occur in the undisturbed forest and are caused by natural gaps in the forest canopy. As noted in Table 2, at two forested sites used as control areas, these gaps average 100 to 200 square metres in area and are mostly isolated, discrete features. The gaps within the slide coalesce and thus grow larger as movement increases. Therefore, many of the commission errors may be eliminated if coarser spatial resolution data are used. Thematic Mapper Simulator data with a resolution of about 30 metres was obtained of this site and will be analyzed to evaluate this effect.

The maximum-likihood classifier is also able to separate the slow and moderate movement zones within the slide by identifying the margins of these zones where extensive differential ground movement has heavily disrupted the canopy and exposed bare soil and/or deciduous vegetation. The fast rate zone is well defined due to the canopy destruction throughout its area. Within both the slow and moderate zones there are some omission "errors" with pixels identified as forest. In reality, these sites may not be true "errors" but correspond to patches or islands of canopy left intact floating on the earthflow. As the slide velocity increases, the canopy islands become smaller and more isolated, and at rates greater than one metre per year the islands are less than 30 metres in minimum dimension. Again, coarser spatial resolution data may improve the cleanness of

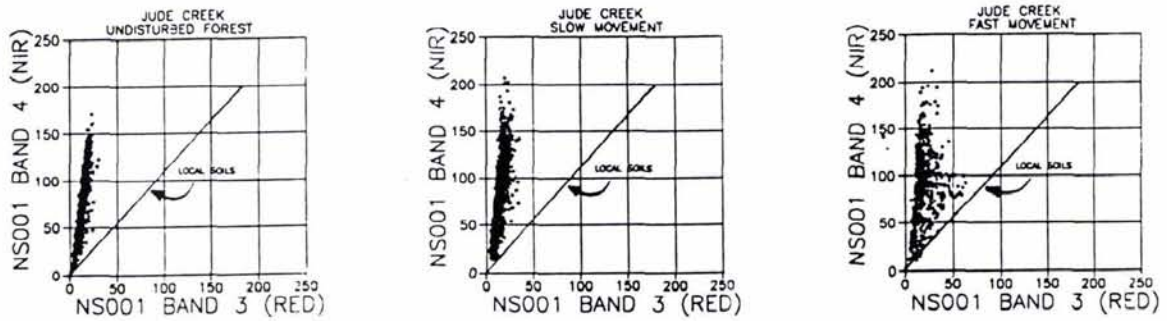

FIG. 11. Jude Creek earthflow reflectance values.

the movement zone classification. It is likely, though, that the position and shape of the canopy islands can be related to the mechanics of the slide movement, and, in that case, preserving them in the classification would be desirable. Work is continuing to assess the effect of coarser resolution data and to quantify the accuracy of classifications of other forested earthflows in the Jude Creek area.

Because disruption of the canopy should increase pixel to pixel contrast, edge density and inertia textural analyses were done on the same NS001 data (See Hlavka (1987) and McKean and Buechel (1990) for descriptions of these methods). Contrast as measured by these textural tests did increase from the undisturbed forest to the earthflow and with movement rate within the earthflow. The textural measures were run on all bands and an example result for the thermal channel (Band 8) is shown in Figure 12. Textural classifiers calculated independently and in conjunction with spectral classifiers will be evaluated to assess their ability to map forested earthflows.

CONCLUSIONS

Remote sensing techniques can be used successfully to map site parameters indicative of potential and existing landslides in some circumstances. Depending on the approach and scale of investigation of slide hazard assessment, the remote sensing input will vary. Vegetation type is recognized as an important variable in the occurrence of shallow landslides through the effect of roots and evapotranspiration. Vegetation mapping can be readily accomplished using remotely sensed data and incorporated as a data layer in a multivariate statistical evaluation of landslide susceptibility. Preliminary results suggest that vegetation does affect debris flow frequency over granitic materials, with the greatest differences occurring within drier aspects. Work is continuing to evaluate the combined effects of vegetation and other variables such as variations in average moisture conditions corresponding to change in slope aspect.

In another hazard assessment approach based on mapping landforms associated with debris flows, remote sensing can be used as an indirect measure of soil depth. Variations in soil depth on the hillslopes studied reflect the local geomorphic processes that are involved in the long-term slope evolution. This evolution includes the formation of relatively thick deposits of colluvium in topographic hollows over a time scale of several thousand years. These deposits are then likely sources of debris flows that will evacuate the hollows during intense storms. The use of an indirect measure to identify the deposits inevitably introduces some uncertainty in the results. However, at the primary Marin County, California test site, near-infrared/red, mid-infrared/infrared, and greeness indices all appear to accurately detect the major colluvial deposits. The indices correlate well with actual soil depths up to a limit of several metres if they are computed for data sets taken late in the growing season. While the indirectness of remote sensing measures is a disadvantage, their synoptic views are a great advantage. This is particularly true when applied to parameters such as soil depth whose spatial variability is otherwise extremely difficult to evaluate.

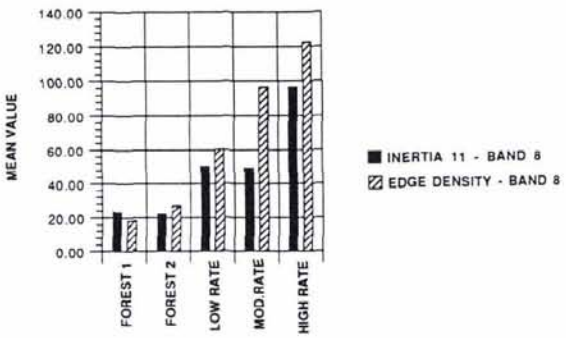

FIG. 12. Jude Creek earthflow texture values.

Multispectral data can also be used in some circumstances to identify and map existing landslides obscured by a forest canopy. In an old-growth coniferous forest, spectral differences appear to be related to the creation of openings in the canopy as the earthflow slowly moves. Exposure of understory vegetation, bare soil, and fallen tree trunks in the canopy openings affects reflectance properties. At Jude Creek, Oregon these spectral effects can be indirectly related to slide movement rate through the degree of canopy disruption that has occurred. Further work is required to test the accuracy of these results and their applicabilty elsewhere.

ACKNOWLEDGMENT

This project was supported by the NASA Earth Science and Applications Division EOCAP program.

REFERENCES

Brabb, E., 1987. Analyzing and portraying geologic and cartographic information for landuse planning, emergency response, and decision making in San Mateo County, CA: *Proc. of GIS Symposium*, American Congress on Surveying and Mapping, American Society of Photogrammetry, pp. 362–374.

Chiariello, N. R., 1989. Phenology of California grasslands: *Grassland Structure and Function, California Annual Grassland*, (L. Huennke and H. Mooney, eds.) Kluwer Academic Publishers, pp. 47–56.

Dengler, L., A. Lehre, and C. Wilson, 1987. Bedrock geometry of unchannelized valleys: *Symp. Erosion and Sedimentation in the Pacific Rim*, Corvallis, Oregon, IAHS Publication 165, pp. 81–90.

Dietrich, W., and T. Dunne, 1978. Sediment budget for a small catchment in mountainous terrain: *Zeitschrift für Geomorphologie*, Supp. 29, pp. 191–206.

Dietrich, W. E., S. L. Reneau, and C. J. Wilson, 1987. Overview: "zero order basins" and problems of drainage density, sediment transport and hillslope morphology: *Symp. Erosion and Sedimentation in the Pacific Rim*, Corvallis, Oregon, IAHS Publication 165, pp. 27–37.

Ellen, S., and G. Wieczorek (eds.), 1988. *Landslides, Floods, and Marine Effects of the Storm of January 3–5, 1982 in the San Francisco Bay Region, CA*. USGS Professional Paper 1434, U.S. Gov. Print. Off., Washington, D.C.

Elvidge, C. D., 1990. Visible and near infrared reflectance characteristics of dry plant materials: *Int. Jour. Remote Sensing*, Vol. 11, No. 10, pp. 1775–1795.

Hack, J. T., and J. C. Goodlett, 1960. *Geomorphology and Forest Ecology of a Mountain Region in the Central Appalachians*: U.S. Geological Survey Prof. Paper 347, 66p.

Hlavka, C., 1987. Land-use mapping using edge density texture measures on Thematic Mapper Simulator data: *IEEE Trans., Geosci. Remote Sensing*, GE-25 (1), pp. 104–108.

Heilman, J. L., and W. E. Boyd, 1986. Soil background effects on the spectral response of a three-component rangeland scene: *Remote Sensing of Environment*, Vol. 19, pp. 127–137.

Huete, A. R., and R. D. Jackson, 1987. Suitability of spectral indices for evaluating vegetation characteristics on arid rangelands: *Remote Sensing of Environment*, Vol. 23, pp. 213–232.

Hunt, E. R., B. N. Rock, and P. S. Nobel, 1987. Measurement of leaf relative water content by infrared reflectance: *Remote Sensing of Environment*, Vol. 22, pp. 429–435.

Kelsey, H. M., 1977. *Landsliding, Channel Changes, Sediment Yield and Land Use in the Van Duzen River Basin, North Coastal California, 1941–1975*: U.S.D.A. Forest Service, Region 5, Earth Resources Monograph 3, 370p.

Mark, R. K., in press. *Map of Debris-Flow Probability, San Mateo County, California*: U.S.G.S. Map I-1257-M.

McKean, J., and S. Buechel, 1990. Remote sensing of forested earthflows: Protecting Natural Resources With Remote Sensing, *Proc. of the Third Forest Service Remote Sensing Applications Conference*, 9–13 April, Tucson, Arizona, American Society for Photogrammetry and Remote Sensing, pp. 198–206.

Miller, G. P., M. Fuchs, M. J. Hall, G. Asrar, E. T. Kanemasu, and D. E. Johnson, 1984. Analysis of seasonal multispectral reflectances of small grains: *Remote Sensing of Environment*, Vol. 14, pp. 153–167.

Reneau, S. 1984. *Depositional and Erosional History of Hollows: Applications to Landslide Location and Frequency, Long-Term Erosion Rates, and the Effects of Climatic Change*: Unpublished Ph.D. Dissertation, University of California at Berkeley, 327p.

Schuster, R. L., 1978. Introduction: *Landslides, Analysis and Control*, (R.L. Schuster and R.J. Krizek, eds.), Transportation Research Board Special Report 176, National Academy of Sciences, Washington, D.C., pp. 1–10.

Swanson, F.J., and M.E. James, 1975. *Geology and Geomorphology of the H.J. Andrews Experimental Forest, Western Cascades, Oregon:* U.S.D.A. Forest Service, Research Paper PNW-188, 14 p.

Vogelmann, J. E., and B. N. Rock, 1986. Assessing forest decline in coniferous forests of Vermont using NS-001 Thematic Mapper Simulator data: *Int. J. Remote Sensing*, Vol. 7, No. 10, pp. 1303–1321.

Wilson, C. J., 1988. *Runoff and Pore Pressure Development in Hollows*: Unpublished Ph.D. Dissertation, University of California at Berkeley, 284p.